

UCRL-CONF-221925



LAWRENCE  
LIVERMORE  
NATIONAL  
LABORATORY

# Isochoric implosions for fast ignition

D. S. Clark, M. Tabak

June 9, 2006

29th European Conference on Laser Interaction with Matter  
Madrid, Spain  
June 11, 2006 through June 16, 2006

## **Disclaimer**

---

This document was prepared as an account of work sponsored by an agency of the United States Government. Neither the United States Government nor the University of California nor any of their employees, makes any warranty, express or implied, or assumes any legal liability or responsibility for the accuracy, completeness, or usefulness of any information, apparatus, product, or process disclosed, or represents that its use would not infringe privately owned rights. Reference herein to any specific commercial product, process, or service by trade name, trademark, manufacturer, or otherwise, does not necessarily constitute or imply its endorsement, recommendation, or favoring by the United States Government or the University of California. The views and opinions of authors expressed herein do not necessarily state or reflect those of the United States Government or the University of California, and shall not be used for advertising or product endorsement purposes.

# Isochoric implosions for fast ignition

Daniel S. Clark<sup>1</sup>, Max Tabak<sup>1</sup>

<sup>1</sup> *Lawrence Livermore National Laboratory, P.O. Box 808, L-015, Livermore, CA 94551, USA*

## ABSTRACT

Fast Ignition (FI) exploits the ignition of a dense, uniform fuel assembly by an external energy source to achieve high gain. In conventional ICF implosions, however, the fuel assembles as a dense shell surrounding a low density, high-pressure hotspot. Such configurations are far from optimal for FI. Here, it is shown that a self-similar spherical implosion of the type originally studied by Guderley [Luftfahrtforschung **19**, 302 (1942).] may be employed to implode a dense, quasi-uniform fuel assembly with minimal energy wastage in forming a hotspot. A scheme for realizing these specialized implosions in a practical ICF target is also described.

## 1. Introduction

Fast Ignition (FI) (Tabak et al., 1994) offers an exciting alternative to the conventional hotspot ignition approach to Inertial Confinement Fusion (ICF) (Lindl, 1998). In the conventional approach, it is the accumulation and stagnation of the hydrodynamic flows at the center of the imploding capsule which produces the extreme temperatures and pressures necessary for fusion ignition. By contrast, for FI, an external energy source, such as the highly energetic electrons produced in intense laser-plasma interaction or laser-generated beams of protons (Roth et al., 2001), is injected into the dense fuel assembly to initiate fusion reactions. Since the fuel assembly and fuel ignition steps are thereby separated in FI, significantly higher gains and more robust targets are projected to be feasible over the conventional scheme.

While considerable attention has been focused on the beam-plasma interactions integral to FI, *i.e.*, electron beam generation from relativistic laser-plasma interaction, the propagation of such beams in dense plasmas, or charged particle stopping in near-Fermi degenerate plasmas, relatively little attention has so far been given to the accompanying hydrodynamics of FI implosions. This omission is especially noteworthy given that, with their externally supplied ignition sources, FI implosions optimize with different imploded fuel configurations than their conventional counterparts. In particular, while the conventional approach is fundamentally dependent on the formation of a robust hotspot to ignite, this central hotspot is a liability in FI. Since ignition occurs effectively from the outside of the fuel assembly in FI, the fusion burn wave in a FI target would propagate predominantly around the edge of the fuel assembly where the fuel density is high. In a high aspect ratio hotspot implosion, this would amount to nearly two-dimensional burn front propagation. It is evident that if a near-uniform density, or isochoric, fuel assembly could be arranged, the burn wave would propagate much more efficiently through

the fuel, namely directly through the center of the implosion in a more three-dimensional manner. Figure 1 schematically contrasts these hotspot and quasi-isochoric fuel assemblies in FI.

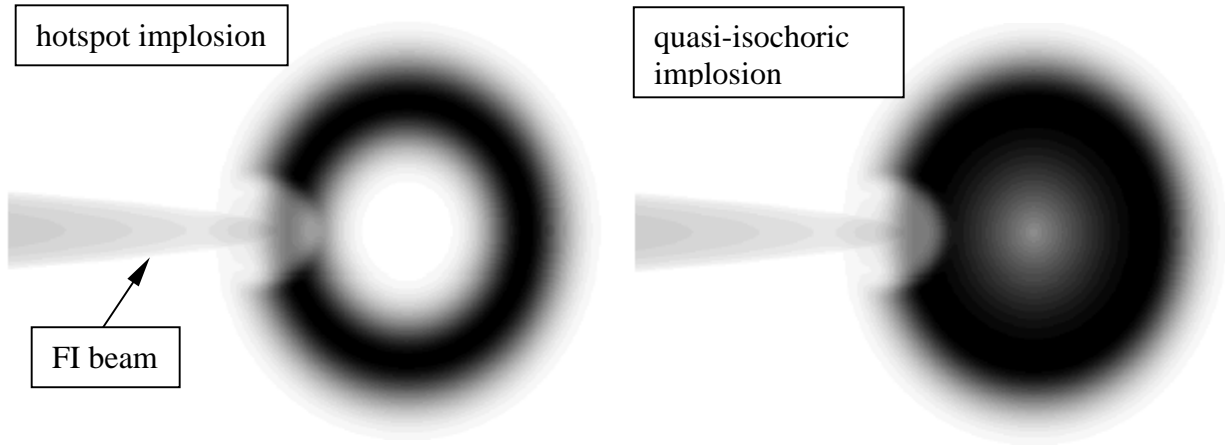


**Figure 1.** Schematic comparison of fast ignition of a typical hotspot implosion and a quasi-isochoric implosion.

Somewhat more quantitatively, it can readily be shown that, for an isochoric implosion and a hotspot implosion of the same peak density and imploded mass (a rough surrogate for implosions requiring the same hydrodynamic energy investment), the areal density (integrated  $\rho r$ ) of the isochoric implosion is higher by the aspect ratio of the hotspot implosion to the two-thirds power. This could be a factor of several for typical hotspot implosions. As a consequence, higher burn fractions can be expected in FI isochoric assemblies than in their hotspot counterparts. Indeed, the gain models which have been proposed for FI target design (and cited to demonstrate its advantages over conventional hotspot ignition) typically assume a near uniform spherical assembly as a starting point (Atzeni, 1999; Tabak, et al. 2006). A challenge, then, in realizing the potential of FI as pointed to by these gain models, is whether and how such quasi-isochoric implosions can be realized.

In the arena of ICF design and theory, a salient role has been played by the class of solutions characterized by self-similarity. The Taylor-Sedov blast wave (Taylor, 1950; Sedov, 1959) and the self-similar nonlinear heat wave (Zel'dovich & Razier, 1967) are two particularly prominent examples from quite disparate areas of ICF-related research. As implied by their name, these specialized solutions have the property of remaining similar to themselves: that is, translations in space or time amount simply to a rescaling of some fundamental solution whose essential shape is invariant. (They are often also referred to as auto-models for the same reason.) Mathematically, this similarity property has the highly convenient effect of reducing systems of partial differential equations depending on both space and time variables into ordinary differential equations depending on only a single self-similar variable.

Historically, solutions of this type have been viewed primarily as idealizations of the real flows which might occur in practice. That is, for a particular flow of interest, the very strong constraint of self-similarity is unlikely to be satisfied exactly; nevertheless, the flow might be sufficiently close to self-similarity to make such an approximation useful. As such, these exact self-similar solutions have been utilized primarily for extracting generalized scaling laws to

describe broad families of implosions (Kidder, 1974; Kemp & Meyer-ter-Vehn, 2001) or as test problems for validating hydrodynamics computer codes. A peculiarity of these solutions, however, is that a particular sub-family of solutions represents the implosion of a spherical shell into a nearly uniform density imploded core. Such an implosion is precisely the isochoric assembly sought as a FI target. Noting this property, the objective of this paper is to use these self-similar implosions as a guide in designing a quasi-isochoric FI target. The challenge for FI implosion design becomes, then, the challenge of developing a strategy for realizing one of these specialized self-similar flows. Given that no phase of a self-similar implosion can correspond to the shell being at rest, the necessary starting point of any real implosion, the essential difficulty is then not to identify that such self-similar implosions exist but to determine a strategy for reaching this self-similar state with practicable implosion parameters.

As an aside, it should be noted that “duding” the capsule hotspot by introducing a high-Z gas into the capsule void, and so radiating away the hotspot energy, has also been proposed as a technique for producing quasi-isochoric implosions (Slutz & Herrmann, 2003). While this is certainly a viable alternative scheme, it has, however, yet to be shown in simulations that a genuinely isochoric assembly can be achieved in this way. The penalty of “poisoning” the capsule central region from useful fusion burn is also obvious. Furthermore, the introduction of a high-Z gas, such as xenon, into the center of a cryogenic capsule entails certain technical challenges of its own. For these reasons, this scheme will not be addressed further here. In a similar vein, it may also be noted that there exist self-similar implosions which transform uniform density solid spheres into uniform density solid spheres of arbitrarily high density (Ferro-Fontan et al., 1975). While this would appear to make for a particularly simple target design, reaching the densities of interest by this scheme appears to require untenably high driving pressures. Hence, only shell-based self-similar implosions are considered here.

This paper is organized as follows. The following section reviews the mechanics and mathematics of self-similar spherical implosions as laid out in the work of Guderley and many others. That a subset of these self-similar implosions yields a quasi-isochoric core after stagnation is noted. Section 3 then addresses the central challenge of accessing such specialized, self-similar implosions from the practical initial condition of a stationary spherical shell. A carefully-timed, multi-step implosion history is found to be necessary. Section 4 then renders this multi-step implosion in the form of a one-dimensional (1-D) idealized implosion design that fits within the parameter space of realistic laser powers, shell aspect ratios, etc. Section 5 concludes.

## 2. Self-Similar Shell Implosions

Since Guderley's pioneering work on the problem of spherically and cylindrically imploding shock waves (Guderley, 1942), considerable study has been dedicated to the field of self-similar gas dynamics, particularly in the context of spherical explosions or implosions. A particularly encyclopedic account of these solutions is given by Lazarus (Lazarus, 1981), and his notation is adopted here. The essential ingredient in all of these self-similar spherical solutions is the *Ansatz*, first made by Guderley, that the radial and temporal dependence of the flow enters only through the single quantity  $x = t/r^\lambda$ , subsequently referred to as the self-similar variable.

With this *Ansatz*, comes the necessary decomposition of the dimensional flow variables, radial velocity, sound speed, and density, respectively, according to

$$u(r,t) = -(r/\lambda t)V(x) \quad (1a)$$

$$c(r,t) = -(r/\lambda t)C(x) \quad (1b)$$

$$\rho(r,t) = r^\kappa R(x) \quad (1c)$$

Here,  $\lambda$  and  $\kappa$  are numerical parameters and the dimensionless reduced functions  $V(x)$ ,  $C(x)$ , and  $R(x)$  are to be determined. Substituting these expressions into the 1-D spherical Euler equations for adiabatic compressible gas flow reduces that system of three coupled nonlinear partial differential equations to two nonlinear ordinary differential equations and one perfect integral:

$$\frac{dC}{dV} = \frac{F[V, C(V)]}{G[V, C(V)]} \quad (2a)$$

$$\frac{d \ln x}{dV} = \frac{D[V, C(V)]}{G[V, C(V)]} \quad (2b)$$

$$\text{const.} = \left(\frac{C}{x}\right)^2 R^{1-\gamma} [(1+V)R]^{[\kappa(\gamma-1)+2(\lambda-1)]/(\kappa+3)} \quad (2c)$$

where  $F(V,C)$ ,  $G(V,C)$ , and  $D(V,C)$  are algebraic functions of their arguments. An ideal gas equation of state is assumed and  $c^2 = \gamma p/\rho$ . Below, the ratio of specific heats  $\gamma$  will always be taken to be 5/3.

The technique for solving Eqs. (2), and hence the 1-D Euler equations, is to integrate Eq. (2a) for the function  $C(V)$  (numerically if necessary), and with that solution then integrate Eq. (2b) for  $x(V)$ . The latter function may then be inverted to determine  $V(x)$  and from that  $C(x) = C[V(x)]$ . The reduced density as a function of the self-similar variable  $R(x)$  is then known from the integral, Eq. (2c). With all three reduced variables determined as functions of  $x$ , Eqs. (1) and the definition  $x = t/r^\lambda$  then give the solution of Euler's equations in  $r$  and  $t$ . What remains to constrain the fundamental solution  $C(V)$  is that the physical solutions  $u(r,t)$ ,  $c(r,t)$ , and  $\rho(r,t)$  satisfy the boundary conditions of the problem at hand. For the implosion of a hollow shell, these conditions are that the pressure (and hence sound speed) and the density of the fluid go to zero at the shell inner edge and that the velocity of the flow go to zero at  $r = \infty$ . In the  $V$ - $C$  plane in which the solution of Eq. (2a) is sought, this means that the solution curve must connect the points  $(V,C) = (-1,0)$  and  $(0,0)$ , corresponding to the shell inner edge and  $r = \infty$ , respectively. Note that this choice of boundary points sets the velocity scale of the problem to be the velocity at the shell inner edge.

The crucial step in this solution process is the inversion of the function  $x(V)$  for  $V(x)$ . From Eq. (2b), this is seen to be possible provided the function  $G(V,C)$  remains non-zero. It is the case, however, that  $G(V,C)$  is zero all along the singular line  $C = 1+V$ , a line which must be

crossed by the solution curve in progressing from  $(V,C) = (-1,0)$  to  $(0,0)$ . The only way in which this line may be crossed and the solution remain single-valued (*i.e.*, physical) in  $x$  is to cross at a singular point where  $D(V,C)$  is zero as well. This is the fundamental constraint on the solution  $C(V)$  which determines the allowed values of  $\lambda$  and  $\kappa$ .

The above procedure outlines the self-similar solution of the Euler equations for the in-going phase of the implosion. For the stagnation or out-going phase of the implosion, the solution curve of Eq. (2a) in the  $V$ - $C$  plane may simply be continued through the point  $(V,C) = (0,0)$  to positive  $V$  (*i.e.*, outward-flowing velocities). Again, however, reaching the proper physical boundary condition necessitates crossing a singular line in the  $V$ - $C$  plane, in this case  $C = -1-V$ . Since there are no suitable points where  $D(V,C)$  is zero with positive  $V$ , single-valuedness in the solution of Eq. (2b) now requires that this singular line be crossed in a discontinuous jump. Physically, this jump corresponds to the return shock which reverses the flow velocity from in-going to out-flowing at the stagnation time.

Figure 2 illustrates a sample self-similar solution trajectory, shown as the red curve, in the  $V$ - $C$  plane. The singular line  $C = 1 + V$ , shown in blue, is crossed at the singular point  $P$  and the green line denotes

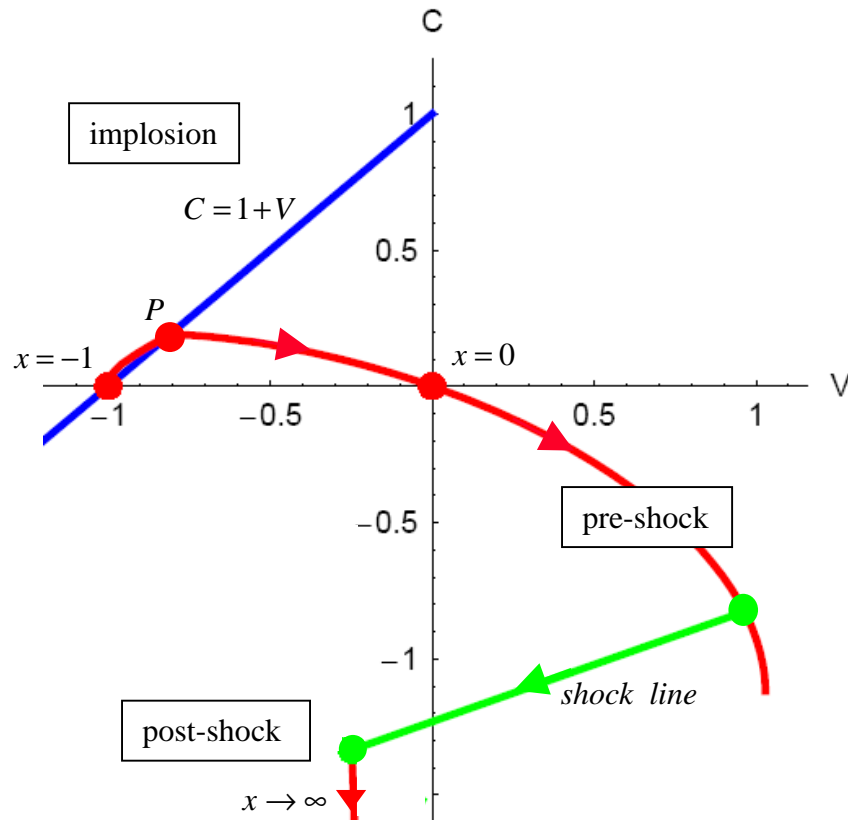


**Figure 2.** Sample self-similar implosion solution in the  $V$ - $C$  plane.

the shock jump. As is customary, the implosion phase of the flow is assigned to  $t < 0$ , and the stagnation phase to  $t > 0$ .  $t = 0$  labels the time of void closure. The self-similar variable has been

scaled to be  $x = -1$  at the leading edge of the shell. From its definition,  $x = 0$  corresponds to the boundary  $r = \infty$  or to the entire shell at  $t = 0$ , and  $x \rightarrow \infty$  corresponds to  $t \rightarrow \infty$  for finite  $r$ . Physically, the solution in the upper left quadrant of the  $V$ - $C$  plane between  $x = -1$  and  $x = 0$  traces out the profile of the imploding shell. The lower half of the  $V$ - $C$  plane, traced from  $x = 0$  to  $x = \infty$ , gives the stagnation phase flow from pre- to post-shock states.

While Eqs. (2) must in general be integrated numerically, certain asymptotic properties of the solutions can yet be obtained analytically (Meyer-ter-Vehn & Schalk, 1982). Specifically, the asymptotic behavior of the physical solutions in the limit  $x \rightarrow \infty$  is given by:

$$u(r,t) = \frac{\mu + \kappa r}{\lambda v \gamma t} \quad (3a)$$

$$\rho(r,t) \sim r^q t^{(q-\kappa)/\lambda} \quad (3b)$$

$$T(r,t) \sim r^{-q} t^{-(\mu+q/\lambda)} \quad (3c)$$

$$p(r,t) \sim r^0 t^{-(\mu+\kappa/\lambda)} \quad (3d)$$

with

$$q = 2 \frac{\kappa(\gamma-1) - 2(\lambda+1)}{2\gamma + \kappa + 2(\lambda+1)} \quad (4a)$$

$$\mu = 2(1+1/\lambda) \quad (4b)$$

$$v = 2\gamma + \kappa + 2(\lambda+1) \quad (4c)$$

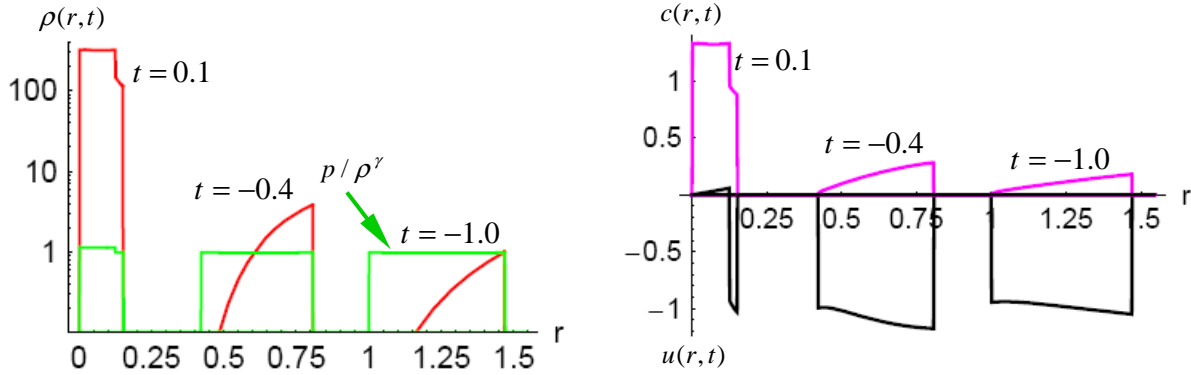
This limit is of particular interest since, from the definition of the self-similar variable  $x$ , it is evident that these limits give either the late time behavior of the flow,  $t \rightarrow \infty$ , or the flow close to  $r = 0$  after void closure. This is precisely this region in space and time that is of greatest interest in target design, *i.e.*, the assembled fuel configuration. Hence, from Eq. (3b), the essential prescription for arranging an isochoric self-similar implosion can be read off: the density  $\rho(r,t)$  will become asymptotically flat if the implosion is driven in such a way that the exponent  $q = 0$ . Equivalently, for a given  $\lambda$ , this requires  $\kappa = 2(1-\lambda)/(\gamma-1)$ .

Figure 3 plots the flow profiles for a self-similar implosion with the parameter  $\lambda = 1.06$ ,  $\kappa = -0.18$ , and hence  $q = 0$  for  $\gamma = 5/3$ . The red curves give the fluid density at the three selected times, the black curves the shell velocity profiles, and the magenta curves the corresponding sound speeds. The implosion of the initially low density shell into a high-density, quasi-isochoric assembly is clearly evident. The discontinuities in the density and velocity profiles at  $t = 0.1$  indicate the location of the return shock. A near factor of 300 increase in density is achieved at the breakout time of this return shock.

Also shown in the figure, as green curves, are the corresponding normalized adiabats  $p/\rho^\gamma$  at each time. As the figure indicates, this flow is not only adiabatic but also isentropic aside from the location of the return shock. This is the distinguishing characteristic of self-similar flows with  $q = 0$ : for  $q > 0$ , the adiabat increases toward the inner edge of the shell and ultimately leads to the formation of a hotspot; for  $q = 0$ , the adiabat is flat through the shell and no hotspot forms.



The physical reason for the formation of an isochoric assembly is also made clear by these adiabats: since the flow stagnates in a nearly isobaric state (see Eq. (3d)), if the flow is arranged also to be isentropic at stagnation, then its final state must perforce be isochoric as well. In detail, when  $q = 0$ , the self-similar inflow of material meeting the return shock is configured precisely such that, even though the shock should weaken as it expands radially, the radially decreasing density which it traverses acts to strengthen the shock and exactly compensate its weakening



**Figure 3.** Flow profiles for a self-similar isochoric implosion with  $\lambda = 1.06$ ,  $\kappa = -0.18$ , and for  $\gamma = 5/3$ .

from expansion. Since the shock is then maintained at a constant strength, the adiabat and pressure, and therefore also the density, are left with nearly constant values behind it.

Isentropic implosion solutions of this type are, in fact, well-known from a context very different from FI: the isentropic collapse of cavitation bubbles in an infinite liquid. This problem was one of the first in fluid mechanics to be addressed self-similarly in the classic solution by (Rayleigh, 1917) and later along the lines of Guderley's method by (Hunter, 1960). In this case, however, the problem was merely to determine the time asymptotic dynamics of bubble collapse assuming the flow to be isentropic. That the isentropic flow after stagnation is also isochoric was an unremarked side effect. In the context of FI implosion designs, these roles are reversed, and this latter property becomes the driving motivation.

As already noted, the existence of self-similar implosion solutions of the type shown in Figure 3 in effect only shifts the problem of designing an isochoric implosion. While these solutions demonstrate that such isochoric assemblies are in fact possible, there remains the problem of initiating such implosions. In practice, an implosion must begin from a shell of a uniform density and at rest. As illustrated in Figure 3, the starting point for these self-similar implosions,  $t = -1$ , is both far from rest and from a uniform density. (The particular value  $t = -1$  is, of course, immaterial since, by its very nature, the solution can be scaled in space and time to start at any particular time and any desired radius.) The fact that the flow must be arranged with a uniform adiabat also augurs that considerable care will be required in designing the implosion so as not to disrupt the initially uniform adiabat. The remainder of this paper develops a method for solving this problem in order to realize the self-similar isochoric state pictured in Figure 3.

Before proceeding to this design of an isochoric target implosion, it is worth noting a remaining general property of these self-similar solutions. Within this field of self-similar gas dynamics, considerable importance has been attached to the notion that self-similar solutions are not merely mathematically convenient curiosities but represent uniquely stable solutions in the space of all possible solutions (self-similar and non-self-similar) to the gas dynamic equations. More importantly, these solutions are generally believed to be attractor solutions in the space of all solutions to which other solutions, beginning for example from non-self-similar initial conditions, tend asymptotically. This concept is central in the theory of intermediate asymptotics (Barenblatt & Zel'dovich, 1972; Barenblatt, 1979). While the attracting nature of these solutions has been much discussed, the proof of this property remains incomplete at best. (Häefele, 1955a & 1955b) has addressed the problem in planar gas flow, and (Lazarus, 1982) has made a linear analysis of the stability of solutions around the various singular points in the  $V$ - $C$  plane for the spherical case. Some progress in this arena was also made by the simulation work of (Thomas et al., 1986).

Though a rigorous proof that self-similar solutions do behave as attractors remains elusive, the concept does offer encouragement to the task of arranging a self-similar isochoric implosion. It is a tautology that self-similar flows always remain similar to themselves. A direct consequence, however, is that it would be impossible to match exactly the flow profiles of a self-similar flow to the profiles of the non-self-similar flow that must result from any practical initial state. Nevertheless, if it is sufficient merely to approximate a self-similar state at some point during the implosion and the flow afterwards will then tend automatically toward self-similarity, the task becomes a feasible one. Indeed, the original analysis of isentropic bubble collapse assumed self-similarity to apply only infinitesimally close to the bubble inner edge and at times infinitesimally close to the time of total collapse. The vast bulk of the flow was assumed not to be self-similar but also not to break the similarity of the flow close to the collapse point. In the design to follow, the self-similar phase will in fact prove to be only the final phase of an otherwise non-self-similar implosion.

### **3. Initiating Self-Similar Implosions from a Stationary Shell**

Any practical ICF implosion begins from an initial shock. This shock is the inevitable consequence of the discontinuous switching on of the laser or other driving beam, but serves the useful purpose of shocking the fuel, generally taken to be DT ice of density 0.25 g/cc, into a near Fermi-degenerate plasma. As is typical of ICF implosions, an initial shock of  $\sim 1.0$  Mbar is assumed here. Following such a shock, the fuel density is  $\sim 1.0$  g/cc, the flow velocity is  $\sim 1.0$  cm/ $\mu$ s, and the plasma may reasonably be approximated as an ideal gas, thus justifying the use of a  $\gamma = 5/3$  ideal gas in the self-similar regime. The flow velocity set by this shock also establishes the time scale of the implosion.

In typical ICF implosions, a train of three shocks is launched into the fuel with each timed so as to overtake the others simultaneously with their breakout from the shell inner edge. While this scheme, in principle, leaves the entire shell on the same adiabat and raises the fuel density to  $\sim 4.0$  g/cc, it requires extremely precise timing of the pressure pulse. Any mistiming in the launching of these shocks, causing one shock to overtake another prematurely or one shock to break out ahead of the others, leads to substantial increases in the adiabat at the inner edge. Such

increases in the adiabat, though undesirable, are not catastrophic for an implosion which is designed ultimately to form a hotspot. If a hotspot is to be avoided, however, as for an isochoric implosion, such mistimings can be ill afforded. Hence, while a multi-shock scheme is theoretically compatible with a totally isentropic implosion, the design below is constrained to a single initial shock. This constraint proves not unacceptably to limit the final imploded density but does significantly enhance the robustness of the design.

Following the break out of the initial shock, a rarefaction wave travels back into the shell at the post-shock sound speed. Once this rarefaction reaches the outer edge of the shell, isentropic flow profiles in density, pressure, and velocity will have been established throughout the shell. These profiles, with the velocity peaked at the inner edge at three times the post-shock sound speed and a sound speed increasing linearly from the inner to outer shell edges, are, however, far from the self-similar profiles pictured in Figure 3. In addition, the Mach number of the shell, limited to  $M \leq 3.3$  for a simple shock-rarefaction flow of an ideal gas, is substantially below that typical in self-similar implosions. A scheme for accessing the self-similar regime other than this simple shock-rarefaction flow is evidently required.

It has already been emphasized that care will be needed in designing an implosion constrained to be entirely isentropic. From the perspective of prescriptive design, however, this constraint of entirely isentropic flow in fact proves to be something of a boon. In this early phase of the implosion, when the shell aspect ratio  $A = R_{in} / (R_{out} - R_{in})$  is large compared to unity and before the shell has converged substantially, it is adequate to work in the planar approximation. In this case, the planar isentropic flow of an ideal gas, an essentially complete and prescriptive theoretical treatment of the flow is available in the form of characteristics and their associated Riemann invariants (Courant & Friedrichs, 1948).

Using these tools of the Riemann invariants and characteristics, it is possible to calculate the flow profiles which result from any given boundary conditions in pressure or velocity, provided the flow is driven sufficiently weakly that no shocks are formed, *i.e.*, isentropy is preserved. Since, in the absence of shocks, the equations are time-reversible, this process itself may be reversed. That is, given a desired future state of the flow, it is possible to calculate explicitly what boundary conditions are necessary to reach that state. For the problem at hand, the boundary conditions are the free-flowing rarefaction of the inner shell edge and the pressure pulse being applied to the outer edge. The desired future state is, of course, the velocity profile of an isentropic self-similar implosion. The details of this procedure for programming a future velocity profile involve the 1-D, time-dependent analogue of the hodograph method for 2-D, time-independent isentropic flow and will be described elsewhere. Physically, the method amounts simply to calculating the shape of the isentropic compression wave to be launched from the outer edge of the shell which, when it interacts with the rarefaction propagating from the inner edge, produces a velocity profile that approximates as nearly as possible a corresponding self-similar profile. For a broad range of self-similar implosions, this procedure proves feasible. Figure 4 illustrates three sequential flow profiles in this process of shaping by the shock, compression wave, and interaction flow. Again, the red curves give the density profiles, and the black curves the corresponding velocities.  $\Delta_0$  denotes the initial shell thickness.

The problem remains, however, of reaching the Mach numbers characteristic of useful self-similar implosions. This is effectively the problem of matching the sound speed profile of the self-similar flow once the velocity profile has been matched as above. Since the procedure for matching the velocity profile relies on launching a compression wave into the shell, and hence raises the sound speed concomitant with the velocity, the Mach number in this method can

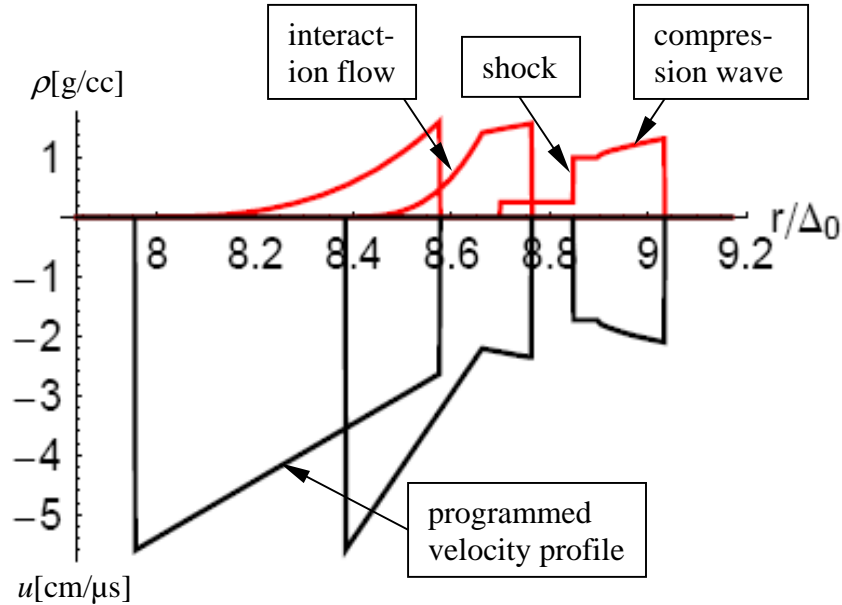


**Figure 4.** Sequential flow profiles illustrating the shaping of the velocity profile by the shock, compression wave, and subsequent interaction flow.  $\Delta_0$  denotes the initial shell thickness.

never be increased to more than  $M \approx 2/(\gamma-1) = 3$ . The solution to this problem is simply to decompress or relax the back of the shell isentropically. A useful way of conceptualizing the pressure history needed for this relaxation is to imagine the pressure experienced by a particle of fluid as it traverses the region of interaction between the compression wave from the shell outer edge and the rarefaction from the inner edge. If the imploding shell extended to infinite radius, the rarefaction from the inner shell edge could continue indefinitely. The fluid particles caught in this infinite rarefaction would then continue to decompress isentropically and indefinitely. By selecting the fluid particle which would represent the physical outer shell edge and applying to it the pressure it would have experience in this fictitious “continued” flow, the remainder of the flow ahead of this particle would proceed as if the rarefaction had never ceased. Hence, the pressure and sound speed at the back of the shell would drop isentropically, and the Mach number can be raised to match the self-similar value. This procedure, in effect, amounts to the isentropic equivalent of a picket pulse.

Like the compression wave used in matching to the self-similar velocity profile, the relaxation pressure history needed to match the sound speed profiles may be calculated exactly in the planar limit. However, given the significant duration of this relaxation phase within the total implosion time, the planar approximation no longer applies and the shell convergence must be taken into account for this phase. A direct means of calculating the relaxation pressure including convergence is simply to simulate numerically precisely the conceptualized flow described

above. That is, a shell several times the intended shell thickness is initialized in the simulation with the velocity and pressure profiles appropriate to the “continued” compression wave. As the compression wave drives the shell inward, the pressure experienced at the physical location of the back of the shell can be recorded and subsequently used to drive the relaxation in a shell of the intended thickness. Note that this concept is in keeping with the overall notion that only the leading edge of the shell and only at late times does the flow tend to self-similarity. Figure 5 illustrates these physical and fictitious “continued” flows in the approach to self-similarity.

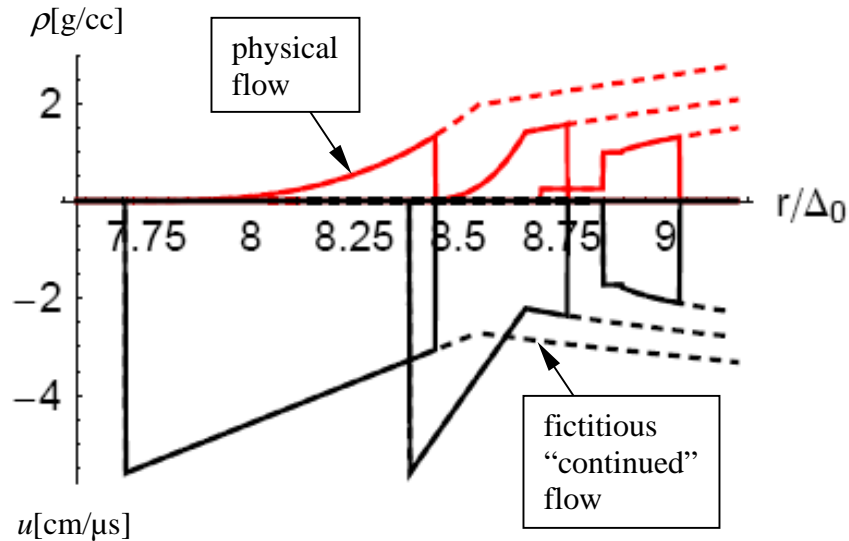


**Figure 5.** Illustration of the physical and fictitious “continued” flows used in raising the shell Mach number isentropically.

### 3. A Quasi-isochoric Target Design

The procedure outlined in the preceding section is sufficient to drive an initially stationary and uniform density shell to an approximately self-similar state. Once this self-similar state is reached, a driving pressure as extracted from the solution described in Section 2 can be applied to the back of the shell, and the final phase of the implosion occurs in a nearly self-similar manner. Combined with the foregoing shock, compression wave, and relaxation phases, such a composite driving pressure pulse is shown in Figure 6. As anticipated, the self-similar phase of the implosion accounts only for approximately the last sixth of the total implosion time. For comparison, the dotted line in the figure also illustrates the relaxation pressure used to raise the shell Mach number but as calculated in the planar approximation. Clearly, this approximation fails dramatically once the shell begins to converge after  $t \approx 5.0 \text{ ns}$   $\Delta_0/100 \text{ }\mu\text{m}$ . The final feature evident in the pressure pulse is that the pressure has been flattopped at 100 Mbar. This is in recognition of the maximum pressure that can likely be achieved in practice. For direct drive with a  $1/3 \text{ }\mu\text{m}$  laser, this corresponds to a laser intensity of  $I \sim 1.3 \times 10^{15} \text{ W/cm}^2$ , or, for indirect drive, to  $T_{\text{rad}} \sim 270 \text{ eV}$ . Continued unchecked the self-similar drive pressure would exceed some thousands of Mbars. Flattopping the pressure, of course, breaks the self-similarity but, as

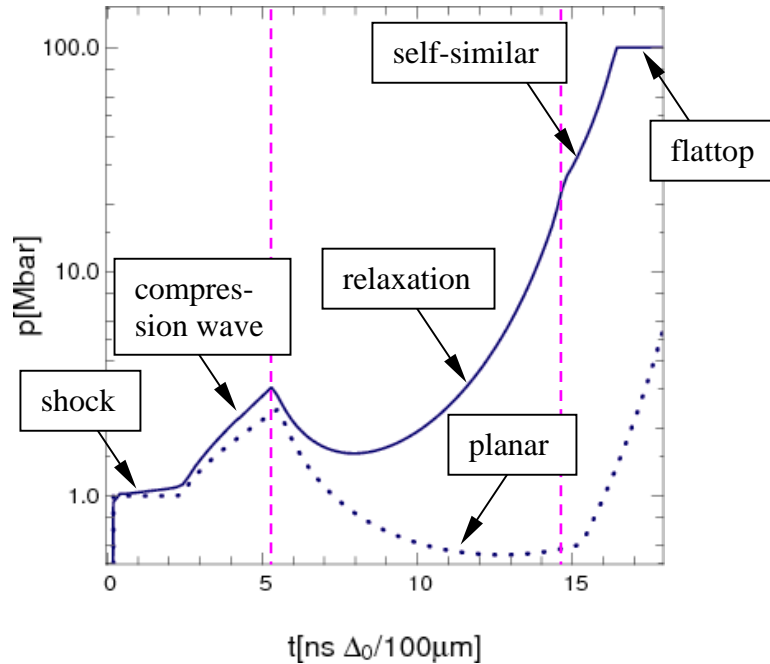


**Figure 6.** Composite pressure history for initiating and driving a self-similar implosion.

illustrated in Figure 9 below, the perturbation introduced by this effect does not unacceptably disrupt the core before the time at which ignition would occur.

The Lagrangian trajectories of the shell inner and outer edges which result from the composite driving pressure are shown in Figure 7. Striking in this plot is the relatively low aspect ratio of the shell ( $A \leq 10$ ) throughout most of the implosion. Coupled with the near constant velocity of the shell through the duration of the implosion, *i.e.*, unaccelerated motion, this implosion can be expected to be particularly stable to Rayleigh-Taylor growth. Figure 8 gives a sequence of flow profiles during the self-similar implosion stage. The simulation results (starting from an initially stationary shell and given by the solid lines) track the desired self-similar flow quite closely.

The final assembled core resulting from this implosion is shown in Figure 9. The assembled density in the simulation (solid line) is in the region of interest for FI ( $\sim 300$  g/cc) but is somewhat less than that in the perfectly self-similar result (dotted line). The assembled mass is also slightly smaller. These are both due in part to the flattopping of the pressure pulse at 100 Mbar as well as the result of some slight mistiming in the pressure drive (since the flow is not perfectly self-similar). Nonetheless, the radial distribution of the density is quite uniform from the center of the implosion to the return shock front. Note that a small hotspot remains in the center of the implosion. This is believed to be a numerical artifact of the treatment of the shock as it breaks out of initial the shell. In a realistic target, however, the inevitable gas which sublimates from the frozen fuel layer and fills the central void will almost invariably produce a similar feature. Optimistically, it might be hoped that any degree of Rayleigh-Taylor mixing in such a small hotspot would be sufficient to smooth away this small void. In either case, the vast bulk of the fuel is of remarkably uniform and high density.

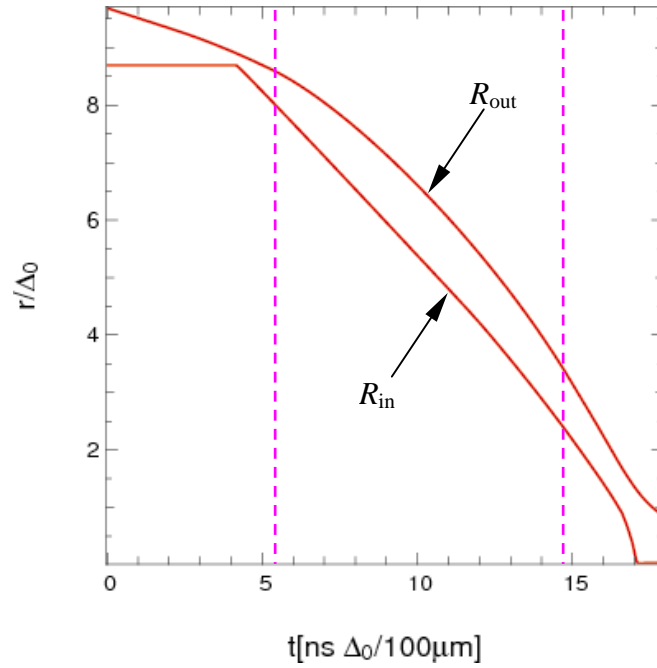


**Figure 7.** Lagrangian trajectories of the shell inner and outer edges which result from the driving pressure shown in Figure 6.

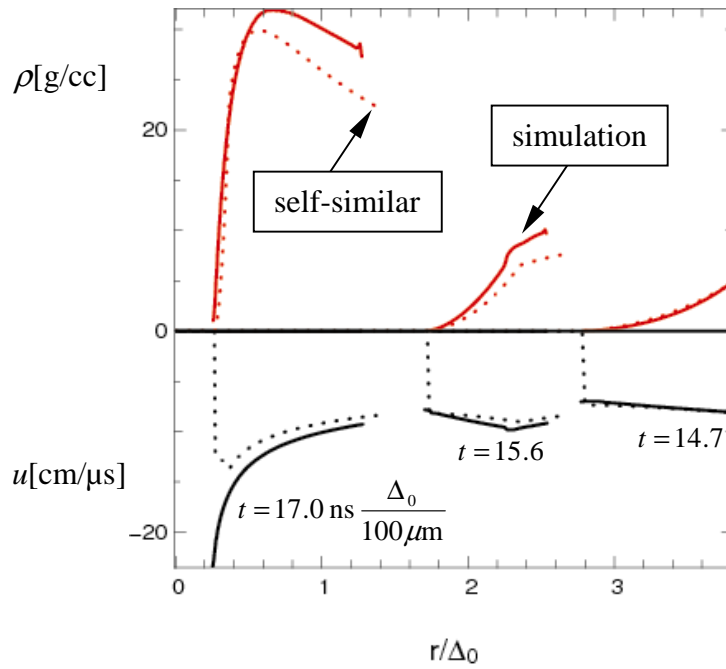


**Figure 8.** Sequential flow profiles during the self-similar phase of the implosion pictured in Figure 7.

Finally, requiring that the assembled core yield an areal density of  $\rho r \sim 3.0 \text{ g/cm}^2$ , the necessary initial shell thickness can be determined from Figure 9 to be  $\Delta_0 \sim 200 \text{ }\mu\text{m}$ . For a target of this size, the invested hydrodynamic energy is the quite reasonable value

$$\varepsilon_{\text{hydro}} = 4\pi \int dt p_{\text{edge}} R_{\text{edge}}^2 \dot{R}_{\text{edge}} \approx 15 \text{ kJ} \quad (5)$$

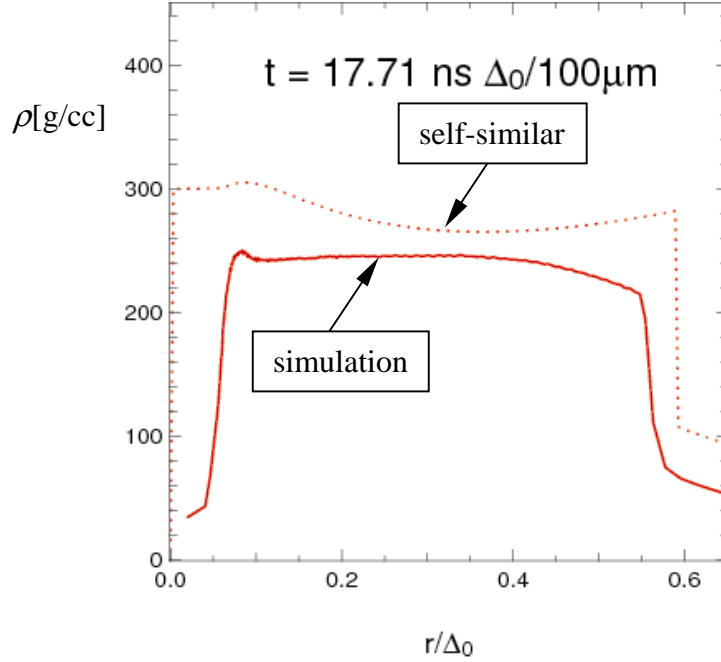


**Figure 9.** Final assembled core resulting from the implosion in Figure 7.

#### 4. Conclusions

The considerations discussed in this paper for preparing an isochoric fuel assembly constitute only the first step in designing such a target. Foremost, the simulation results presented in Section 3 assumed an ideal gas equation of state for the shell and drove the implosion through the idealization of a pressure source applied to the outer edge of the shell. These two simplifications should be replaced in the simulation by using a realistic equation of state and introducing a proper laser or radiation drive. The former can be expected to necessitate slightly modifying the early phase of the pressure pulse but to have little impact on the late phase. With the latter, the complication of the dynamics of the ablator must be added to the target design. Also, as alluded to in Figure 9, the effect of the inevitable gas fill in the central void, though likely very small, deserves investigation.

Despite their simplifying assumptions, the results described in Section 3 seem sufficiently encouraging to motivate further work. This is especially so given the benefits to FI of an isochoric fuel assembly and the potential for very high gains from FI targets.



## 5. References

- ATZENI, S. (1999). Inertial fusion fast ignitor: Igniting pulse parameter window vs the penetration depth of the heating particles and the density of the precompressed fuel. *Phys. Plasmas*. **6**, 3316–3326.
- BARENBLATT, G.I. & ZEL'DOVICH, Ya.B. (1972). Self-similar solutions as intermediate asymptotics. *Ann. Rev. Fluid Mech.* **4**, 285–312.
- BARENBLATT, G.I. (1979). *Similarity, Self-similarity, and Intermediate Asymptotic*. New York: Consultants Bureau.
- COURANT, R. & FRIEDRICHS, K.O. (1948). *Supersonic Flow and Shock Waves*. New York: Springer.
- FERRO-FONTAN, C., GRATTON, J. & GRATTON, R. (1975). Self-similar spherical implosions. *Phys. Lett. A*. **55**, 35–37.
- GUDERLEY, G. (1942). Strong spherical and cylindrical shock fronts near the center of the sphere or cylinder axis. *Luftfahrtforschung*. **19**, 302–312.
- HÄEFELE, W. (1955a). Zur analytischen Behandlung ebener, starker, instationärer Stoßwellen. *Z. Naturforsch.* **10a**, 1006–1016.
- HÄEFELE, W. (1955b). Über die Stabilität des Stoßwellentypus aus der Klasse der Homologie-Lösungen. *Z. Naturforsch.* **10a**, 1017–1027.
- HUNTER, C. (1960). On the collapse of an empty cavity in water. *J. Fluid Mech.* **8**, 241–263.
- KIDDER, R.E. (1974). Laser compression of matter: optical power and energy requirements. *Nuc. Fusion*. **14**, 797–803.
- LAZARUS, R.B. (1981). Self-similar solutions for converging shocks and collapsing cavities. *SIAM J. Num. Anal.* **18**, 316–370.
- LAZARUS, R.B. (1982). One-dimensional stability of self-similar converging flows. *Phys. Fluids*. **25**, 1146–1155.
- LINDL, J.D. (1998). *Inertial Confinement Fusion: the Quest for Ignition and Energy Gain Using Indirect Drive*. New York: American Institute of Physics.
- MEYER-TER-VEHN, J. & SCHALK, C. (1982). Selfsimilar spherical compression waves in gas dynamics. *Z. Naturforsch.* **37a**, 955–969.
- LORD RAYLEIGH. (1917). On the pressure developed in a liquid in the collapse of a spherical cavity. *Phil. Mag.* **34**, 94–98.

ROTH, M., COWAN, T.E., KEY, M.H., et al. (2001). Fast ignition by intense laser-accelerated proton beams. *Phys. Rev. Lett.* **86**, 436–439.

SEDOV, L.I. (1959). *Similarity and Dimensional Methods in Mechanics*. New York: Academic Press.

SLUTZ, S.A. & HERRMANN, M.C. (2003). Radiation driven capsules for fast ignition fusion. *Phys. Plasmas*. **10**, 234–240.

TABAK, M., HAMMER, J., GLINSKY, M.E., et al. (1994). Ignition and high gain with ultrapowerful lasers. *Phys. Plasmas*. **1**, 1626–1634.

TABAK, M., HINKEL, D., ATZENI, S., et al. (2006). Fast ignition: overview and background. *Fusion Sci. & Technology*. **49**, 254–277.

TAYLOR, G. (1950). The formation of a blast wave by a very intense explosion, *Proc. Royal Soc. London*. **201a**, 159–174.

THOMAS, L.P., PAIS, V., GRATTON, R. & DIEZ, J. (1986). A numerical study on the transition to self-similar flow in collapsing cavities. *Phys. Fluids*. **29**, 676–679.

ZEL'DOVICH, Ya.B. & RAIZER, Yu.P. (1967). *Physics of Shock Waves and High-Temperature Hydrodynamic Phenomena*. New York: Academic Press.

This work was performed under the auspices of the U. S. Department of Energy by University of California, Lawrence Livermore National Laboratory under contract W-7405-Eng-48.